ICP Imperial College Press
www.icpress.co.uk

ANALYSIS OF DYNAMIC AND ACOUSTIC RADIATION CHARACTERS FOR A FLAT PLATE UNDER THERMAL ENVIRONMENTS

QIAN GENG and YUEMING LI*

*State Key Laboratory for Strength and
Vibration of Mechanical Structures
Xi'an Jiaotong University
Xi'an 710049, China
liyueming@mail.xjtu.edu.cn

A study on vibration and acoustic radiation characters of an isotropic rectangular thin plate under thermal environments is presented in this paper. It is assumed that thermal loads caused by thermal environments just change the structure stress state. Thermal stresses induced by uniform temperature rise of the plate are determined with the thermo-elastic theory. Then the stress state is used in the following dynamic analysis as a pre-stressed factor. It is observed that thermal loads influence the natural frequencies evidently, especially the fundamental natural frequency. The order of mode shapes stays the same. Dynamic response peaks float to lower frequency range with the increment of structure temperature. Acoustic radiation efficiency of the plate subjected to thermal loads decreases in the mid-frequency band. For validation, numerical simulations are also carried out. It can be found that the combined approach of finite element method (FEM) and boundary element method (BEM) is more appropriate for radiation problems.

Keywords: Isotropic rectangular thin plate; thermo-elastic analysis; pre-stressed vibration; acoustic radiation; thermal environment.

1. Introduction

In modern aerospace exploration, structures not only absorb various loads, but also work under many different environments like thermal and moisture. These factors will affect the performance and stability of structures.

In service, spacecraft usually works in an extreme condition of high ambient temperature and the structure is heated seriously [Behrens and Muller, 2004]. Temperature changes caused by the thermal environment change will make a number of impacts on the material properties, structure configuration and the stress state and so on. The early researches of structure dynamic characters under thermal

---

*Corresponding author.

environment may date back to more than 50 years ago [Boley, 1956; Boley and Barber, 1957]. Jadeja and Loo [1974] investigated thermally induced vibration of rectangular plates subjected to a sinusoidal heat flux and an approximate solution with double trigonometric series was given. They found that the inertia terms are very important for heated plate. Ganesan and Dhotarad [1984] employed numerical methods to study the vibration behavior of thermally stressed plates. In their work, FEM was used in thermal stress analysis, and finite difference technique and variational approach were applied in dynamic analysis. Shu *et al.* [2000] analyzed the free vibration of clamped circular plates with coupling temperature and stress field. Yeh [2005] studied the large deflection vibration of a simply supported orthotropic plate with thermo-mechanically coupled effect. It is found that the thermo-mechanical coupling effect performed as thermo-elastic damp causes a decay of vibration amplitude and the coupling effect must be considered when the initial deflection is large. Kim [2005] developed a theoretical method to investigate the vibration of functionally graded rectangular plates under thermal environments. Thermal stresses and temperature-dependent material properties were considered in the study. The results confirmed that material compositions, plate geometry and temperature rise influence the vibration behavior significantly. Amabili and Carra [2009] presented a study of nonlinear forced vibration of a plate computationally and experimentally. They found that temperature variations and geometric imperfections play important roles. Recently, Brischetto and Carrera [2011] investigated the free vibration of one-layered and two-layered metallic plates using a fully coupled thermo-mechanical model.

The first study of sound radiation from structures was carried out by Rayleigh in 1896. He derived the Rayleigh integral to calculate the far-field acoustic response. With the development of mechanical technology, acoustic radiation from vibrating structures has been of great interest to researchers and engineers since the middle of 20th century [George, 1961; David, 1961; Richard, 1962; Maidanik, 1962]. In aerospace industry, noise generated from structures will affect the mechanical environment of space vehicles and might be harmful to human beings working with the facilities [Wilby, 1996]. As the groundwork for noise control, the acoustic radiation characters of simple structures are analyzed widely. A statistical method was proposed to estimate the acoustic response of a ribbed panel in the whole frequency range by Maidanik [1962]. It is found that the ribbing increases the radiation resistance. A good agreement between the theory and experiments was obtained. Wallace [1972] studied the radiation resistance associated with natural modes of a finite rectangular panel using the total energy radiated. Asymptotic solutions were derived in low frequency range, and a waviness of radiation resistance was observed below the critical frequency. Williams [1983] used a series expansion in ascending powers of wave number for acoustic power to investigate the radiation from baffled and unbaffled planar sources. He studied rectangular plates with various boundary conditions and pointed out that the volume flow across the surface must be zero.

Radiation characters of finite thin structures with general elastic boundary conditions were studied using the variational formulation by Atalla *et al.* [1996]. It is found that baffles have very important effect at low frequency range. Xie *et al.* [2005] investigated the average radiation efficiency of plates and strips and found that the radiation efficiency of strips below the fundamental frequency is proportional to the square of the shorter edge length. Putra and Thompson [2010] calculated the sound radiation from a perforated plate and obtained that the radiation efficiency reduces with the increment of perforation ratio and the size reduction of the hole at a certain perforation ratio.

With the increasing importance of the thermal environment of space vehicles, the structural dynamic and acoustic radiation characters considering the thermal effect bring about some new problems. Jeyaraj *et al.* [2008, 2009] investigated vibration and acoustic response of isotropic and composite plate under thermal environments with combined FEM and BEM. They found that the natural frequencies decrease with an increase of the temperature applied on the plate while vibration response and sound radiation increase. Kumar *et al.* [2009] carried out parametric studies on vibro-acoustic response of FGM elliptic disc under thermal environments with commercial software. It is obtained that the vibration response increases suddenly when the thermal load increase from 0.25 to 0.5 times critical buckling temperature. Besides the articles above, there are not yet many studies on this topic and the existing researches are almost based on numerical simulations.

In this paper, structural dynamic and acoustic radiation characters under the thermal environments are analyzed theoretically, and numerical simulations are also employed as validation. The vibration of an isotropic rectangular thin plate in the pre-stressed state due to the change of thermal environment is studied. The influence of membrane forces induced by thermal loads on dynamic response is considered. And then, the radiation character of the thermally stressed plate is investigated. The material properties are temperature-independent.

2. Theoretical Model

Consider a rectangular thin plate simply supported on each edge vibrating in the air domain as shown in Fig. 1. The plate is lying in the plane $z = 0$ with dimensions a in the x-direction, b in the y-direction and h in the thickness. The acoustic medium occupies the half-infinite space ($z > 0$). The plate is assumed to be vibrating under thermal environments.

2.1. *Plate under thermal environments*

Assume that the plate is stress-free at the reference temperature T_0. When the structure temperature changes to T, stress state of the plate will be changed by the resulting thermal stresses. If the temperature change across the thickness is uniform, the thermo-elastic problem of plate can be described with plane stress state. The
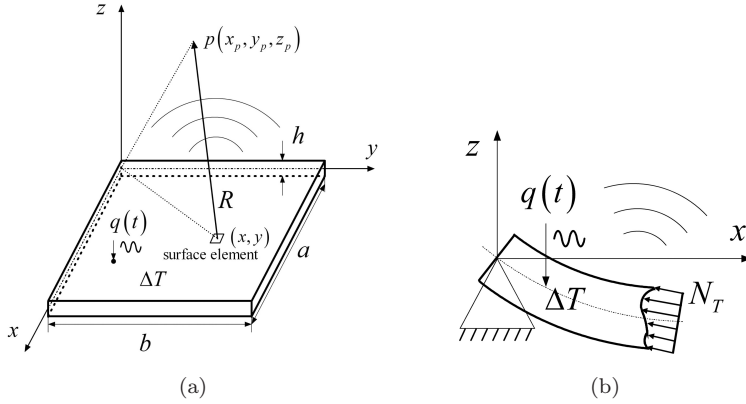
Fig. 1. Scratch of the radiating plate: (a) global view, and (b) cross-section view.

stress–displacement relations will be [Hetnarski and Eslami, 2008]

$$\sigma_x = \frac{E}{1-v^2}\left[\left(\frac{\partial u}{\partial x} + v\frac{\partial v}{\partial y}\right) - (1+v)\alpha\Delta T\right], \tag{1}$$

$$\sigma_y = \frac{E}{1-v^2}\left[\left(\frac{\partial v}{\partial y} + v\frac{\partial u}{\partial x}\right) - (1+v)\alpha\Delta T\right], \tag{2}$$

$$\sigma_{xy} = \frac{E}{2(1+v)}\left(\frac{\partial u}{\partial y} + \frac{\partial v}{\partial x}\right), \tag{3}$$

where u and v are the in-plane displacements, E and v are the Young's modulus and the Poisson's ratio of plate material respectively, α is the thermal expansion coefficient, and $\Delta T = T - T_0$ is denoted as the temperature change.

In the present study, the thermal environment is assumed to induce a uniform temperature rise in planewise in the plate. Taking the boundary condition into account, the thermal load here will not cause in-plane displacement. Then Eqs. (1)–(3) will be simplified into

$$\sigma_x = -\frac{E\alpha\Delta T}{1-v}, \tag{4}$$

$$\sigma_y = -\frac{E\alpha\Delta T}{1-v}, \tag{5}$$

$$\sigma_{xy} = 0, \tag{6}$$

and the membrane forces can be obtained by integrating Eqs. (4)–(6) along the thickness, expressed as follows:

$$N_x = -\frac{\alpha E\Delta T h}{1-v}, \tag{7}$$

$$N_y = -\frac{\alpha E \Delta T h}{1 - \upsilon}, \tag{8}$$

$$N_{xy} = 0. \tag{9}$$

2.2. Vibrating plate under thermal environments

Considering the membrane forces, the governing equation of flexural motion of a rectangular thin plate subjected to transverse loads is given by Dickinson [1971]

$$D_0 \nabla^4 w + \rho h \frac{\partial^2 w}{\partial t^2} = N_x \frac{\partial^2 w}{\partial x^2} + N_y \frac{\partial^2 w}{\partial y^2} + 2N_{xy} \frac{\partial^2 w}{\partial x \partial y} + q, \tag{10}$$

where $D_0 = Eh^3(1+j\eta)/12(1-\upsilon^2)$ is the flexural rigidity of plate, η is the material loss factor which takes damping into account [Pritz, 1998], ρ is mass density, w is the transverse displacement, q is the transverse mechanical load applied on plate, j is the imaginary unit. In this study, the membrane forces are induced by thermal load on the plate and assumed to be constant which can be evaluated with Eqs. (7)–(9).

The out-of-plane displacement at any location on the plate can be found by superposing the modal contributions from each mode of structural vibration of the plate as

$$w(x, y, t) = \sum_{m,n} w_{mn} \phi_{mn}(x, y) e^{j\omega t}, \tag{11}$$

where m and n are mode indices, w_{mn} is the amplitude of mode displacement of the (m, n) mode, and $\phi_{mn}(x, y)$ is the mode shape function. For the simply supported boundary condition, the shape function of rectangular plate takes the following form

$$\phi_{mn}(x, y) = \sin \frac{m\pi x}{a} \sin \frac{n\pi y}{b}. \tag{12}$$

By applying the weighted residual (Galerkin) method, the integral of a weight residual of mode shape function should be set to zero

$$\iint_\Omega \left[D_0 \nabla^4 w + \rho h \frac{\partial^2 w}{\partial t^2} - \left(N_x \frac{\partial^2 w}{\partial x^2} + N_y \frac{\partial^2 w}{\partial y^2} + 2N_{xy} \frac{\partial^2 w}{\partial x \partial y} \right) - q \right]$$
$$\cdot \phi_{mn}(x, y) \mathrm{d}A = 0. \tag{13}$$

To simplify Eq. (13) and solve the mode displacement, substitute Eqs. (7)–(9), (11) and (12) into Eq. (13), and use the orthogonality properties of the mode shape as

$$\iint_\Omega \left(D_0 \phi_{kl}(x, y) \nabla^4 \phi_{mn}(x, y) \right.$$

$$\left. - \phi_{kl}(x, y) \left(N_x \frac{\partial^2}{\partial x^2} + N_y \frac{\partial^2}{\partial y^2} + 2N_{xy} \frac{\partial^2}{\partial x \partial y} \right) \phi_{mn}(x, y) \right) \mathrm{d}A$$

$$= \omega_{mn}^2 \iint_\Omega \rho h \phi_{kl}(x, y) \phi_{mn}(x, y) \mathrm{d}A = \begin{cases} \omega_{mn}^2 & m = k \quad \text{and} \quad n = l, \\ 0 & m \neq k \quad \text{or} \quad n \neq l. \end{cases} \tag{14}$$

The amplitude of mode displacement can be expressed as

$$w_{mn} = \frac{Q_{mn}}{\omega_{mn}^2 - \omega^2}, \tag{15}$$

where Q_{mn} is the orthogonalized force, ω is the frequency of applied load, ω_{mn} is natural frequency of the (m, n) mode as

$$\omega_{mn} = \sqrt{\pi^4 \left(\frac{m^2}{a^2} + \frac{n^2}{b^2} \right)^2 \frac{D_0}{\rho h} + \frac{N_x}{\rho h} \left(\frac{m\pi}{a} \right)^2 + \frac{N_y}{\rho h} \left(\frac{n\pi}{b} \right)^2}. \tag{16}$$

The out-of-plane displacement of the plate will be stated as

$$w(x, y, t) = \sum_{m,n} \frac{Q_{mn}}{\omega_{mn}^2 - \omega^2} \sin \frac{m\pi x}{a} \sin \frac{n\pi y}{b} e^{j\omega t}, \tag{17}$$

and the out-of-plane velocity of the plate can be evaluated as

$$v(x, y, t) = \sum_{m,n} v_{mn} \phi_{mn}(x, y) e^{j\omega t}, \tag{18}$$

where v_{mn} is the complex amplitude of mode velocity of the (m, n) mode and can be obtained by

$$v_{mn} = \frac{j\omega Q_{mn}}{\omega_{mn}^2 - \omega^2}. \tag{19}$$

2.3. *Far-field acoustic radiation*

The far-field acoustic radiation associated with the vibrating plate can be calculated with Rayleigh integral [Fahy and Gardonio, 2007]. Using the vibration velocity obtained by Eq. (18), the sound pressure radiated from vibrating plate at a point in acoustic field can be expressed as

$$p(x_p, y_p, z_p, t) = \frac{j\omega \rho_a}{2\pi} e^{j\omega t} \int_{\Omega} \frac{\sum_{m,n} v_{mn} \phi_{mn}(x, y) \cdot e^{-jkR}}{R} dA, \tag{20}$$

where ρ_a is air density, $R = \sqrt{(x_p - x)^2 + (y_p - y)^2 + z_p^2}$ is the distance between the observation point (x_p, y_p, z_p) in acoustic field and the integration point (x, y) on the plate, k is the wave number which is evaluated by the load frequency ω and the sound speed c_0 by $k = \omega/c_0$.

3. Example Results and Discussion

In this section, the formulations derived previously are used to calculate the vibration and the sound radiation characters of a simply supported rectangular thin plate, and the influence of thermal environment is studied. The plate is modeled with the geometric size as 0.4 m and 0.3 m in x- and y-direction respectively, and 0.01 m in thickness. Aluminum, with Young's modulus 70 GPa, Poisson's ratio 0.3, mass

density $2700\,\mathrm{kg/m^3}$, thermal expansion coefficient 2.3e-5/K and loss factor 0.001, is chosen as the plate material. The acoustic medium is modeled as air with the density $1.21\,\mathrm{kg/m^3}$ and the sound speed $343\,\mathrm{m/s}$. The material properties are regarded as temperature-independent in this study.

The effect of thermal environments is assumed to change the plate temperature uniformly in both planewise and the thickness direction. All the thermal load cases are designed below the critical buckling temperature. The critical buckling load of plates compressed in two perpendicular directions can be obtained by Timoshenko and Gere [1985]

$$N_x \frac{m^2\pi^2}{a^2} + N_y \frac{n^2\pi^2}{b^2} = -D_0 \left(\frac{m^2\pi^2}{a^2} + \frac{n^2\pi^2}{b^2} \right)^2. \tag{21}$$

Substituting Eqs. (7) and (8) into Eq. (21), the critical buckling temperature of plate can be evaluated with

$$T_{cr} = \frac{h^2\pi^2}{12(1+\upsilon)\alpha} \left(\frac{1}{a^2} + \frac{1}{b^2} \right). \tag{22}$$

For the plate model described above, the critical buckling temperature is about $47.7°\mathrm{C}$. Therefore, five load cases are chosen with uniform temperature rises of $5°\mathrm{C}, 15°\mathrm{C}, 25°\mathrm{C}, 35°\mathrm{C}$ and $45°\mathrm{C}$ respectively, and $0°\mathrm{C}$ is defined as the reference temperature to represent the stress-free state case.

First, natural vibration characters under thermal environments are studied. The first five natural frequencies of the plate under different thermal loads are listed in Table 1, and the mode shapes are stated in brackets. It is clear that the natural frequencies decrease with the increase of the plate temperature while the mode shapes stay the same. The softening effect of thermal loads on the structure is quite obvious, and the influence of thermal environments on the fundamental frequency is most remarkable.

The frequency ratios, defined by f_T/f_0, are plotted in Fig. 2, where f_T and f_0 are the natural frequencies obtained with thermal loads and under the reference environment ($0°\mathrm{C}$ in this work). The absolute value of the slope of frequency ratio curve of the first natural frequency is much greater than others, and the slope increases more rapidly with the temperature rise. The thermal environment influences the fundamental frequency greatly.

Table 1.   Comparisons of natural frequencies of plate with thermal loads (Hz).

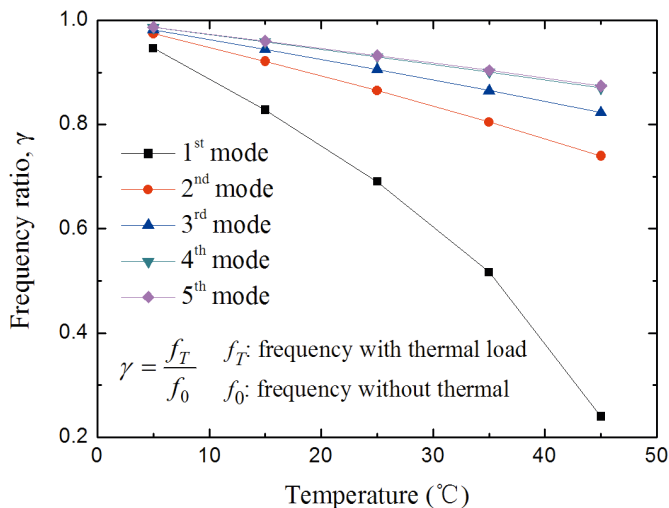| Mode	Thermal load cases					
	$0°\mathrm{C}$	$5°\mathrm{C}$	$15°\mathrm{C}$	$25°\mathrm{C}$	$35°\mathrm{C}$	$45°\mathrm{C}$
1st	420.2(1, 1)	397.6(1, 1)	348.0(1, 1)	290.1(1, 1)	217.2(1, 1)	100.9(1, 1)
2nd	874.0(2, 1)	851.7(2, 1)	805.3(2, 1)	756.1(2, 1)	703.4(2, 1)	646.4(2, 1)
3rd	1227.0(1, 2)	1204.8(1, 2)	1159.1(1, 2)	1111.6(1, 2)	1061.9(1, 2)	1009.8(1, 2)
4th	1630.4(3, 1)	1608.2(3, 1)	1563.0(3, 1)	1516.4(3, 1)	1468.3(3, 1)	1418.6(3, 1)
5th	1680.8(2, 2)	1658.6(2, 2)	1613.4(2, 2)	1566.9(2, 2)	1519.0(2, 2)	1469.5(2, 2)

Fig. 2.   Frequency ratio for the first five natural frequencies.

As the foundation of acoustic radiation, dynamic response of the pre-stressed plate which considering the membrane forces induced by thermal loads is studied. A transverse harmonic point force with amplitude 1N is applied on a proper location of the plate to make sure all the modes below 2000 Hz can be excited.

The temporal and spatial average of square of surface velocity of the plate is calculated under harmonic excitations under different thermal environments, as shown in Fig. 3. For the change of natural vibration under thermal loads, the reduction of natural frequencies and mode shapes invariance, the global characters of velocity
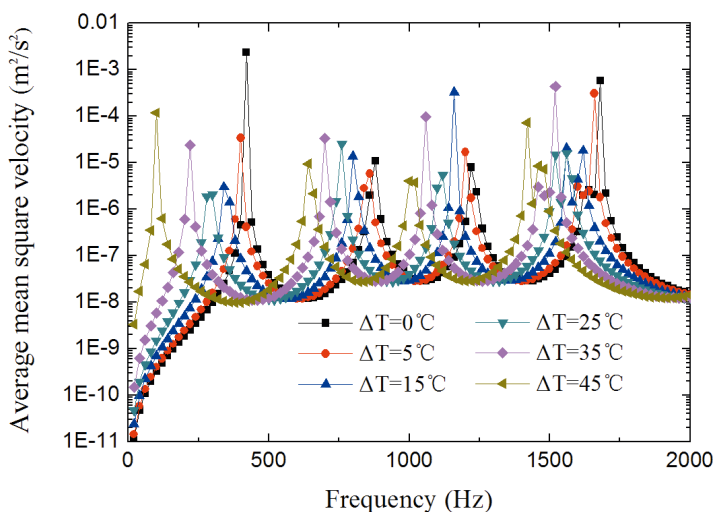

Fig. 3.   Average mean square velocity of the plate under different thermal environments.
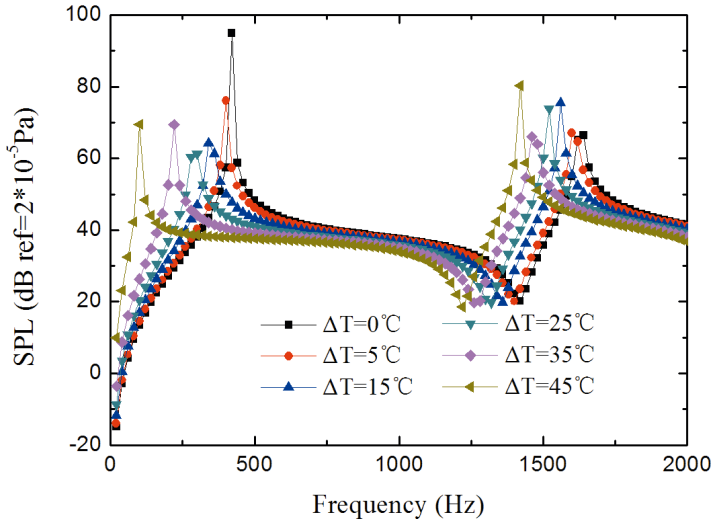
Fig. 4.   SPL at the observation point in acoustic field.

response keep the same, while response peaks float to lower frequency range and the amplitude at the first resonant decreases.

Acoustic radiation is calculated for the vibrating plate. The sound pressure level (SPL) versus the load frequency at a point in the acoustic medium located 3 m off the centroid of the plate is plotted in Fig. 4. As the SPL is influenced by the vibration velocity directly, acoustic radiation has the same trend with velocity response under thermal environments. It can be seen clearly that the resonant frequencies decrease and the SPL responses float to the lower frequency range generally with temperature rise. For the first response peak, related to the first mode of plate, a decrease of the amplitude is obtained with the softening effect under thermal loads.

Figure 5 shows the acoustic radiation power of the plate under thermal environments. In the case of mechanical excitations, the radiated sound from vibrating plate is mainly produced by the structure resonant modes [Norton and Karczub, 2003]. As a result of the natural frequency reduction under thermal environments, the sound radiation power response floats to the lower frequency range showing the same trend with the average mean square velocity. And the amplitude of the first response peak decreases obviously under thermal loads.

Radiation efficiency is the value to describe the radiating effectiveness of structure, obtained by dividing radiation power with acoustic impedance, plate area and surface vibrating velocity [Fahy and Gardonio, 2007]. It is very useful for the estimation of acoustic radiation and noise control [Norton and Karczub, 2003]. Figure 6 shows the radiation efficiency of the vibrating plate below 5000 Hz. The results obtained here compare well with Wallace [1972]. Under different environments, the radiation efficiency curves show the same tendency. The response peaks come out
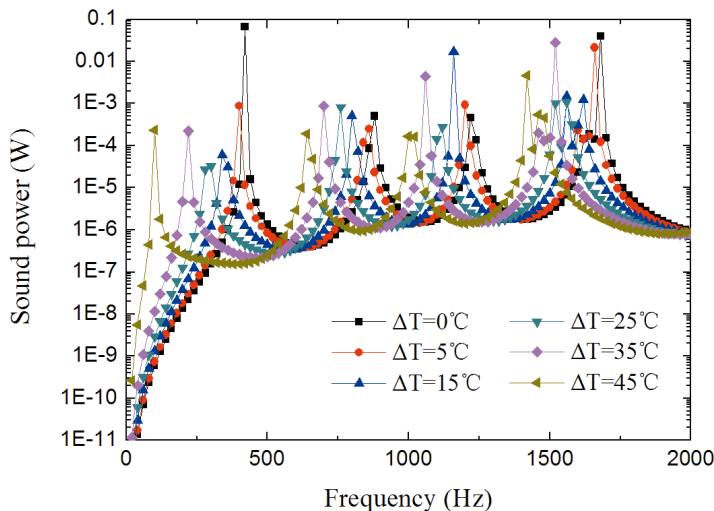
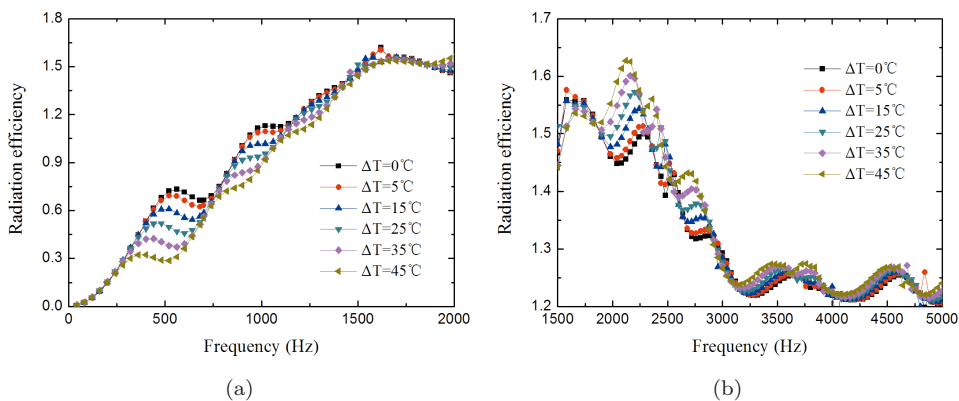Fig. 5. Acoustic radiation power of plate under different thermal environments.

Fig. 6. Radiation efficiency of plate under different thermal environments: (a) frequency domain below 2000 Hz, and (b) frequency domain from 1500 Hz to 5000 Hz.

just above the critical frequency (about 1200 Hz for the plate in this work). Below that value, the efficiency increase gradually and the waviness is quite obvious. Well above the critical frequency, the efficiency curves reduce to unit asymptotically.

Known from the results shown in Fig. 6, thermal loads affect the radiation efficiency of the plate evidently but does not change the global characters. It is clear that there is almost no influence of thermal load on radiation efficiency of plate in low frequency band (below about 250 Hz) under thermal environments, shown in Fig. 6(a). Above that range, the radiation efficiency with considering thermal effect decreases greatly below the critical frequency. At about 500 Hz, the decrement of radiation efficiency for the case with the structure temperature of 45°C, which is

very close to the plate critical buckling temperature, reaches more than half of that value obtained in the reference case (with the structure temperature of 0°C). As the temperature increases, the waviness of radiation efficiency curves become smoother and the first wave comes in lower frequency region. With the increment of load frequency, the differences of efficiency among the thermal load cases reduce rapidly.

At about 1600 Hz, the radiation efficiency without thermal effect reaches peak value and the value keeps the same under thermal environments. In higher frequency region, the radiation efficiency becomes to reduce gradually with the increment of load frequency. It can be seen from Fig. 6(b) that the conversion capability of mechanical energy to radiated sound energy is higher under thermal environments. Especially when the thermal load applied on the plate is much closer to the critical temperature, the radiation efficiency comes out a new peak. In other words, the peak value of radiation efficiency is higher under thermal environment, and it appears at higher frequency range.

4. Validation

Numerical simulations for the same model used in previous section are also employed as validation studies. At first, vibration characters obtained with theoretical solutions of plate under 0°C and 45°C are compared with the results obtained from Abaqus using FEM. The plate is modeled with mesh density of 20×20.

Comparisons of natural frequencies are listed in Table 2 and are visualized in Fig. 7. It can be seen that the values match well except the first natural frequencies under thermal environment. From previous analysis, it is known that thermal environment influences fundamental natural frequency greatly. It is confirmed in this validation study as well. On the one hand, the first natural frequency is much less than higher-order frequencies. So it is more sensitive to membrane forces change. On the other hand, the different methods used to deal with eigenvalue problems in theoretical and numerical analyses result in the differences. However, the results still show the same tendency of softening effect of plate under thermal environment.

Velocity response comparisons at the harmonic excitation point on the plate are plotted in Fig. 8. The response curves show a good agreement. Because of the difference of natural frequencies between the theoretical values and numerical

Table 2. Comparisons of natural frequencies of theoretical and numerical results (Hz).

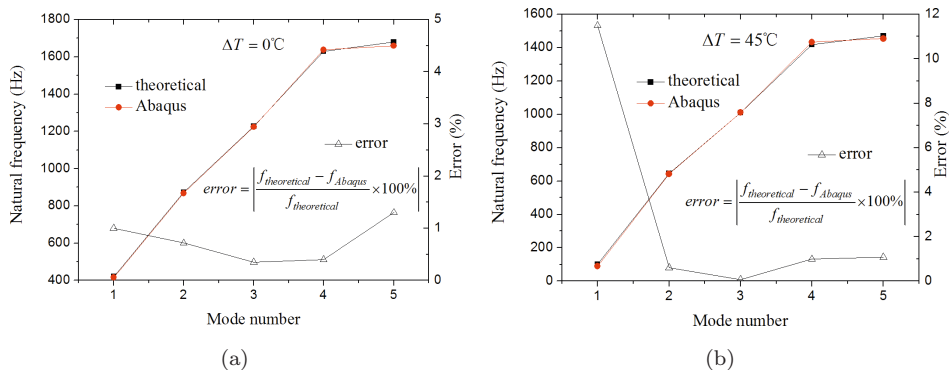| ΔT		Natural frequency (Hz)				
		1st	2nd	3rd	4th	5th
0°C	Theoretical	420.2	874.0	1227.0	1630.4	1680.8
	Abaqus	416.0	867.7	1222.7	1636.9	1658.9
	Error/%	1.00	0.72	0.35	0.40	1.30
45°C	Theoretical	100.9	646.4	1009.8	1418.6	1469.5
	Abaqus	89.3	642.5	1010.5	1432.7	1453.6
	Error/%	11.5	0.60	0.07	0.99	1.08

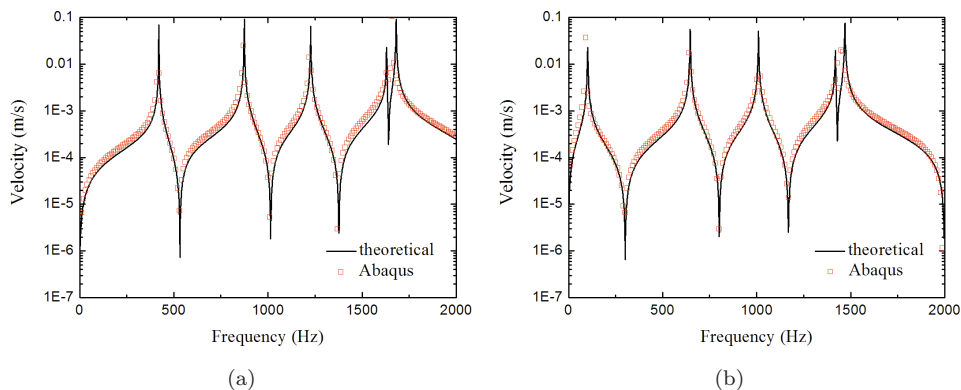Fig. 7.   Comparisons of natural frequencies: (a) $\Delta T = 0°\text{C}$, and (b) $\Delta T = 45°\text{C}$.

Fig. 8.   Velocity response comparisons at the excitation point: (a) $\Delta T = 0°\text{C}$, and (b) $\Delta T = 45°\text{C}$.

results, the response peaks appear a little mismatch. However, the overall dynamic characters of the theoretical results are well accordant with the numerical ones.

Acoustic radiation of plate is calculated with FEM in Abaqus and combined approach of FEM/BEM in VA One. Computational models used here are shown in Fig. 9. In Abaqus, both the plate and the air domain are modeled using FEM meshes. To simulate the infinite domain with the finite elements, the faces of the acoustic meshes are all set as non-reflection boundaries. In FEM/BEM analysis, finite element meshes are used to model the plate, while the BEM fluid is used to simulate the acoustic field. Normal mode results are obtained from MD Nastran with finite element analysis and imported into VA One, and then the structure response and BEM fluid analysis are carried out.

Acoustic radiation responses are compared with the theoretical and the numerical results as shown in Fig. 10. It can be observed that results obtained from VA One show more satisfactory agreement with the theoretical solutions. There are some extra peaks in response curves obtained from Abaqus. In acoustic radiation
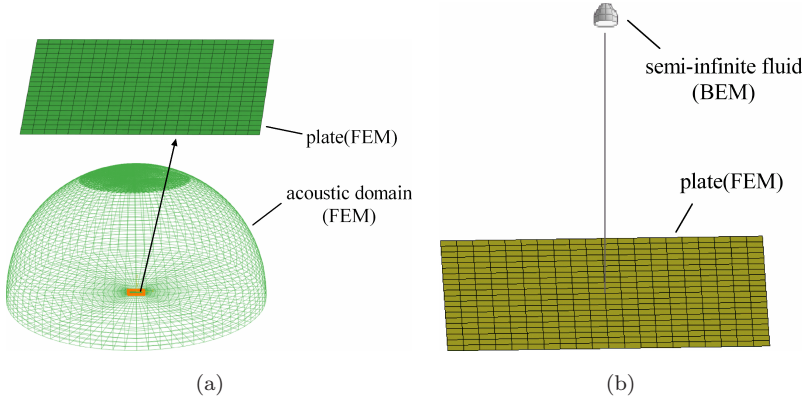
(a) (b)

Fig. 9.   Numerial calculation models used for validation: (a) FEM/FEM model in Abaqus, and (b) FEM/BEM model in VA One.
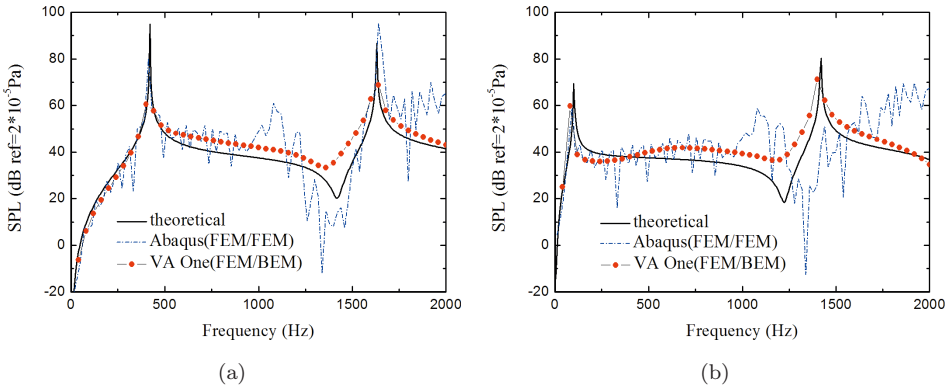

(a) (b)

Fig. 10.   SPL comparisons at the observation point: (a) $\Delta T = 0°\mathrm{C}$, and (b) $\Delta T = 45°\mathrm{C}$.

analyses of vibrating structures with light fluid such as air in this work, which can be considered as sequentially coupled problems, acoustical effects acting on structures are negligible. With Abaqus FEM/BEM (plate/air) simulations, the interaction between structures and acoustic medium is fully considered. The extra response peaks obtained from Abaqus represent the effect of acoustical modes. Acoustic medium is not only perturbed by the vibrating structures, but also produces feed-backs on the structure in FEM/FEM simulation. On the other hand, due to the limitation of the finite number of elements used in FEM simulations, the error in higher frequency band becomes much larger in dynamic analyses. It is clear that the FEM/FEM results appear much higher above the second resonance frequency in Fig. 10. For these reasons mentioned above, the combined approach of FEM/BEM (plate/air) method is better than FEM/FEM simulation for studying the acoustic radiation problems of structures with light fluid.

5. Conclusion

The influence of thermal environments on the dynamic response and acoustic radiation characters are investigated in this paper. Theoretical expressions are first derived for the vibration and acoustic radiation of a simply supported rectangular thin plate with considering the membrane forces induced by thermal environment change. Numerical simulations with FEM/FEM in Abaqus and the combined approach of FEM/BEM in MD Nastran and VA One are also employed to validate the theoretical results.

It is observed that with the uniform structure temperature rise below the critical buckling temperature, the mode shapes stay the same, while the natural frequencies of plate decrease evidently. Especially, the fundamental natural frequency is influenced most greatly. With the change of the natural vibration characters under thermal environments, plate velocity and SPL response peaks float to lower frequency range, however, the global characters of responses do not change.

The radiation efficiency decreases obviously below the critical frequency, and the influence of thermal environment reduces gradually with the increment of load frequency. The waviness of efficiency curves becomes smoother with the increment of structure temperature, and the first wave comes at lower frequency. In the low frequency band (below 250 Hz in this work) and the region near the critical frequency of the plate, thermal effects can be neglected. Above the critical frequency, the radiation efficiency is higher for plate under thermal environments, and the peak value comes at higher frequency range. Thermal environment has the opposite effect on the radiation efficiency below and above the critical frequency. The plate has higher effectiveness to convert mechanical energy into sound radiation energy above the critical frequency under thermal environments.

In the validation study, the theoretical values and the numerical results generally match well. The error of the fundamental natural frequency, which is much sensitive to thermal loads, is larger than others under thermal environment. But the dynamic and acoustic responses show a good agreement between the theoretical and the numerical results. For the acoustic radiation problems of the vibrating structure with light fluid, results obtained with the combined approach of FEM/BEM are more approximate to the theoretical solutions.

The present study will be a base for further researches of more complex objects to estimate the working state under thermal environments. It may be useful to predict the mechanical environment of spacecrafts or other structures to reduce the potential harms to human beings and apparatus. This paper can be a foundation of the system control and optimization design.

References

Amabili, M. and Carra, S. [2009] "Thermal effects on geometrically nonlinear vibrations of rectangular plates with fixed edges," *Journal of Sound and Vibration* **321**(3/5), 936–954.

Atalla, N., Nicolas, J. and Gauthier, C. [1996] "Acoustic radiation of an unbaffled vibrating plate with general elastic boundary conditions," *Journal of the Acoustical Society of America* **99**(3), 1484–1494.

Behrens, B. and Muller, M. [2004] "Technologies for thermal protection systems applied on re-usable launcher," *Acta Astronautica* **55**(3/9), 529–536.

Boley, B. A. [1956] "Thermally induced vibration of beams," *Journal of the Aeronautical Sciences* **23**(2), 179–181.

Boley, B. A. and Barber, A. D. [1957] "Dynamic response of beams and plates," *Journal of Applied Mechanics, Trans. ASME* **24**(3), 413–416.

Brischetto, S. and Carrera, E. [2011] "Thermomechanical effect in vibration analysis of one-layered and two-layered plates," *International Journal of Applied Mechanics* **3**(1), 161–185.

David, C. G. [1961] "Vibration and sound radiation of damped and undamped flat plates," *Journal of the Acoustical Society of America* **33**(10), 1315–1320.

Dickinson, S. M. [1971] "Lateral vibration of rectangular plates subject to in-plane forces," *Journal of Sound and Vibration* **16**(4), 465–472.

ESI Group. VA One 2007, `http://www.esi-group.com/`.

Fahy, F. and Gardonio, P. [2007] *Sound and Structural Vibration: Radiation, Transmission and Response* (Academic Press, Oxford).

Ganesan, N. and Dhotarad, M. S. [1984] "Hybrid method for analysis of thermally stressed plates," *Journal of Sound and Vibration* **94**(2), 313–316.

George, C. [1961] "Sound radiation from prolate spheroids," *Journal of the Acoustical Society of America* **33**(7), 871–876.

Hetnarski, R. B. and Eslami, M. R. [2008] *Thermal Stresses-Advanced Theory and Applications* (Springer, New York).

Jadeja, N. D. and Loo, T. C. [1974] "Heat induced vibration of a rectangular plate," *Journal of Engineering for Industry* **96**, 1015–1021.

Jeyaraj, P., Padmanabhan, C. and Ganesan, N. [2008] "Vibration and acoustic response of an isotropic plate in a thermal environment," *ASME Journal of Vibration and Acoustics* **130**(5), 70510055.

Jeyaraj, P., Ganesan, N. and Padmanabhan, C. [2009] "Vibration and acoustic response of a composite plate with inherent material damping in a thermal environment," *Journal of Sound and Vibration* **320**(1/2), 322–338.

Kim, Y. W. [2005] "Temperature dependent vibration analysis of functionally graded rectangular plates," *Journal of Sound and Vibration* **284**(3/5), 531–549.

Kumar, B. R., Ganesan, N. and Sethuraman, R. [2009] "Vibro-acoustic analysis of functionally graded elliptic disc under thermal environment," *Mechanics of Advanced Materials and Structures* **16**(2), 160–172.

Maidanik, G. [1962] "Response of ribbed panels to reverberant acoustic fields," *Journal of the Acoustical Society of America* **34**(6), 809–826.

MSC Software, MD Nastran 2006, `http://www.mscsoftware.com/`.

Norton, M. P. and Karczub, D. G. [2003] *Fundamentals of Noise and Vibration Analysis for Engineers* (Cambridge University Press, Cambridge).

Pritz, T. [1998] "Frequency dependences of complex moduli and complex Poisson's ratio of real solid materials," *Journal of Sound and Vibration* **214**(1), 83–104.

Putra, A. and Thompson, D. J. [2010] "Sound radiation from perforated plates," *Journal of Sound and Vibration* **329**(20), 4227–4250.

Richard, H. L. [1962] "Sound radiation from a beam attached to a plate," *Journal of the Acoustical Society of America* **34**(9), 1265–1268.

Shu, X. F., Zhang, X. Q. and Zhang, J. X. [2000] "Thermoelastic free vibration of clamped circular plate," *Applied Mathematics and Mechanics* **21**(6), 715–724.

SIMILIA Abaqus, http://www.simulia-china.com/.

Timoshenko, S. P. and Gere, J. M. [1985] *Theory of Elastic Stability* (McGraw-Hill Book Company, Inc., New York).

Wallace, C. E. [1972] "Radiation resistance of a rectangular panel," *Journal of the Acoustical Society of America* **51**, 946–952.

Wilby, J. F. [1996] "Aircraft interior noise," *Journal of Sound and Vibration* **190**(3), 545–564.

Williams, E. G. [1983] "A series expansion of the acoustic power radiated from planar sources," *Journal of the Acoustical Society of America* **73**(5), 1520–1524.

Xie, G., Thompson, D. J. and Jones, C. J. C. [2005] "The radiation efficiency of baffled plates and strips," *Journal of Sound and Vibration* **280**(1/2), 181–209.

Yeh, Y. L. [2005] "The effect of thermo-mechanical coupling for a simply supported orthotropic rectangular plate on non-linear dynamics," *Thin-Walled Structure* **43**(8), 1277–1295.